JACS
JOURNAL OF THE AMERICAN CHEMICAL SOCIETY

ARTICLE

pubs.acs.org/JACS

Structural Transformation of Two-Dimensional Metal−Organic Coordination Networks Driven by Intrinsic In-Plane Compression

Jun Liu,[†] Tao Lin,[‡] Ziliang Shi,[‡] Fei Xia,[†] Lei Dong,[‡] Pei Nian Liu,*[,†] and Nian Lin*[,‡]

[†]Shanghai Key Laboratory of Functional Materials Chemistry and Institute of Fine Chemicals, East China University of Science and Technology, Meilong Road 130, Shanghai, China

[‡]Department of Physics, The Hong Kong University of Science and Technology, Clear Water Bay, Hong Kong, China

ABSTRACT:

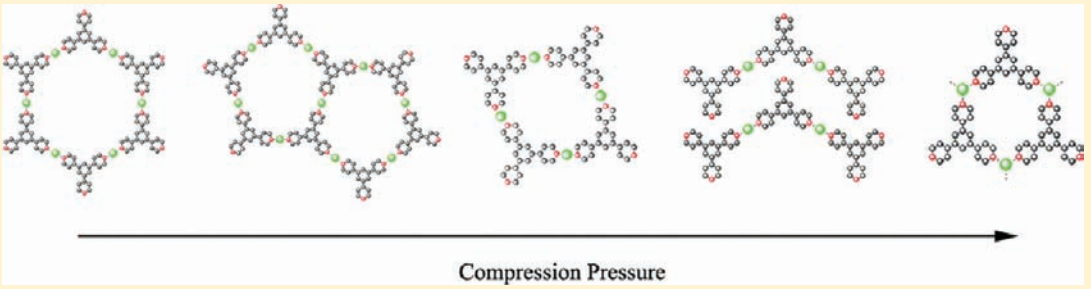

The coordination assembly of 1,3,5-trispyridylbenzene with Cu on a Au(111) surface has been investigated by scanning tunneling microscopy under ultrahigh vacuum conditions. An open two-dimensional (2D) metal−organic network of honeycomb structure is formed as the 2D network covers partial surface. Upon the 2D network coverage of the entire surface, further increment of molecular density on the surface results in a multistep nonreversible structural transformation in the self-assembly. The new phases consist of metal−organic networks of pentagonal, rhombic, zigzag, and eventually triangular structures. In addition to the structural change, the coordination configuration also undergoes a change from the two-fold Cu−pyridyl binding in the honeycomb, pentagonal, rhombic and zigzag structures to the three-fold Cu−pyridyl coordination in the triangular structure. As the increment of molecular packing density on the surface builds up intrinsic in-plane compression pressure in the 2D space, the transformation of the structure, as well as the coordination binding mode, is attributed to the in-plane compression pressure. The quantitative structural analysis of the various phases upon molecular density increment allows us to construct a phase diagram of network structures as a function of the in-plane compression.

INTRODUCTION

Supramolecular systems frequently exhibit structural transformation, that is, different structures are formed under specific external variables, for example, temperature, concentration, pressure, solvent, and so forth.[1,2] In particular, structural transformation of porous metal−organic framework (MOF) structures has attracted increasing interest.[2] Recently, two-dimensional (2D) supramolecular coordination networks assembled on surfaces have been directly observed by scanning tunneling microscopy (STM),[3] thus, providing model systems for investigating the phase transformation mechanisms of coordination self-assembly. In fact, understanding and controlling of the phase transformation in the self-assembled scaffolds of surface-confined molecules afford a unique way to control the structures and properties of 2D metal organic networks,[4−10] which are of fundamental importance in the design of nanostructured materials. Various parameters such as solvent,[5] concentration,[6] temperature,[7] coverage,[8] molecular ratios,[9] electrical stimulation,[10] and guest exchange[11] have been proved effective to induce the phase transformation in the 2D self-assembled supramolecular architectures.

The highly porous MOF structures are extremely flexible and compressible, resulting in considerable sensitivity to applied compression pressure.[12] Very recently, the structural transformation of MOFs induced by compression pressure has been studied in the form of single crystals[13] or powders[14] via hydrostatic compression in a diamond anvil cell filled with a pressure-transmitting medium. Under the pressure up to several gigapascals, the pressure inducing structural transformation and the lattice volume changes were observed by means of high-pressure X-ray diffraction.[13,14] For 2D porous supramolecular structures, however, the structural change under high pressure is inaccessible since the external pressure could not be applied directly toward the 2D systems either in liquid-phase or in ultrahigh vacuum conditions. Here, we report a study which makes use of intrinsic in-plane compression pressure built up by 2D gas phase molecules confined on a surface. We demonstrate that on a Au(111) surface, the self-assembly of molecular ligands of 1,3,5-tris(pyridyl)benzene (TPyB, shown in Figure 1a) with

Received: June 17, 2011
Published: October 10, 2011

dx.doi.org/10.1021/ja2056193 | *J. Am. Chem. Soc.* 2011, 133, 18760–18766

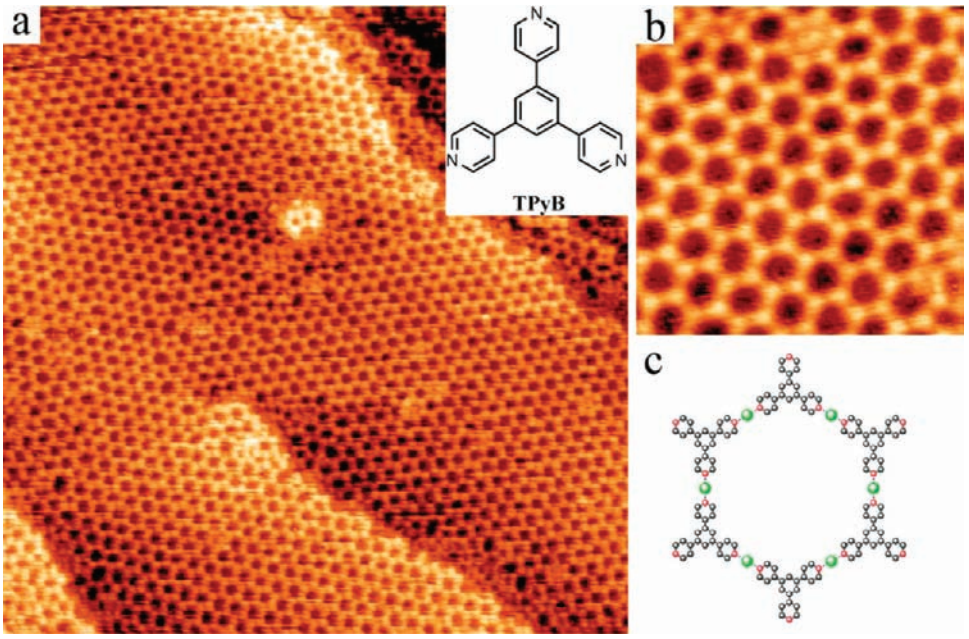

Figure 1. (a) Overview STM topograph (100 nm × 100 nm) of the TPyB−Cu honeycomb networks formed at a molecular density of 0.32 TPyB/nm^2. Inset: chemical structure of TPyB. (b) High-resolution image (20 nm × 20 nm) of the honeycomb network. (c) Structural model of the honeycomb network (Cu in green and N in red).

Cu forms various coordination network structures steered by in-plane compression. The structural characteristics of the various networks and the phase transformation processes are monitored at molecular resolution using STM. Our results shed new lights on the roles that compression plays in 2D coordination self-assembly.

RESULTS AND DISCUSSION

First, we deposit low-dosage TPyB molecules and copper atoms on the Au(111) surface, that is, the adsorbed molecules cover partial surface. Under this condition, a honeycomb network structure is formed.[15] As we continuously increase the TPyB dosage on the surface (the Cu is assured to be always overdosed as evidenced by the presence of extra Cu islands), the honeycomb network gradually covers more surface area. At a TPyB dosage corresponding to a molecular density of about 0.32 TPyB/nm^2, one full monolayer of metal−organic coordination networks (i.e., the surface is fully covered by the networks) is formed on the Au(111) surface. A typical overview STM topography image is shown in Figure 1a revealing highly ordered honeycomb networks with few defects (ca. 8% of TPyB). A high-resolution STM image is shown in Figure 1b with molecular resolution. The neighboring TPyB molecules are arranged in a "corner-to-corner" manner; that is, the neighboring TPyB molecules approach each other with their pyridyl terminal groups. One TPyB molecule can be identified to attach to three neighboring TPyB molecules, thus, constructing the honeycomb lattice. On the basis of the STM data, we propose a model as drawn in Figure 1c. A Cu atom coordinates the neighboring N atoms of the pyridyl groups in a two-fold linear configuration.[16] The Cu atoms are not resolved in the STM data, presumably due to the electronic effect which was reported before.[16,17] The area of one hexagonal unit is 6.5 nm^2 and the densities of Cu atom and TPyB molecule in honeycomb lattice are 0.46 Cu/nm^2 and 0.31 TPyB/nm^2.

In a two-dimensional space, moving adsorbates are in a 2D gas phase, which build up in-plane 2D pressure. The in-plane 2D pressure shares many similar properties with three-dimensional pressure. For example, in correlation to the ideal gas law, $PV = nRT$ (n, the mole number of the substance; R, the ideal gas constant; T, temperature in kelvin; P, pressure), the increment of the density of molecules adsorbed on a surface would result in an enhancement of in-plane pressure for the 2D gas phase. To investigate in-plane compression inducing structural transformation, we gradually increase the molecular density on the surface by depositing additional TPyB molecules stepwisely on the surface. After each step, the sample is annealed at 420 K allowing efficient self-assembly and cooled down to 300 K later for structural characterization using STM. Figure 2a is a typical overview STM topography image of the sample on which the molecular density is increased to 0.34 TPyB/nm^2. This figure shows the total area occupied by the honeycomb networks is reduced (ca. 73% of TPyB), and in addition, a new structure consisting of pentagons appears (ca. 14% of TPyB).[18] So, our strategy does work to induce structural transformation of 2D coordination networks through increasing the density of adsorbed molecules. We propose that the phase transformation is driven by in-plane compression in a way that the new phases can effectively reduce the 2D pressure.

In the high-resolution image of this new phase (see Figure 2b), one can see each pentagon shares its two edges of meta-position with the two neighboring pentagons. In each pentagon, four out of five molecules attach to three neighboring molecules in a "corner-to-corner" manner, whereas the one remaining TPyB only attaches to two neighboring molecules. The pentagons tile one by one and two adjacent pentagons always point to opposite directions to constitute a waved string as highlighted by the frame in Figure 2b. The adjacent strings running in parallel then tile staggeredly, forming the periodic ordered network structure. In a structural model as shown in Figure 2c, one can see that in a

dx.doi.org/10.1021/ja2056193 |J. Am. Chem. Soc. 2011, 133, 18760–18766

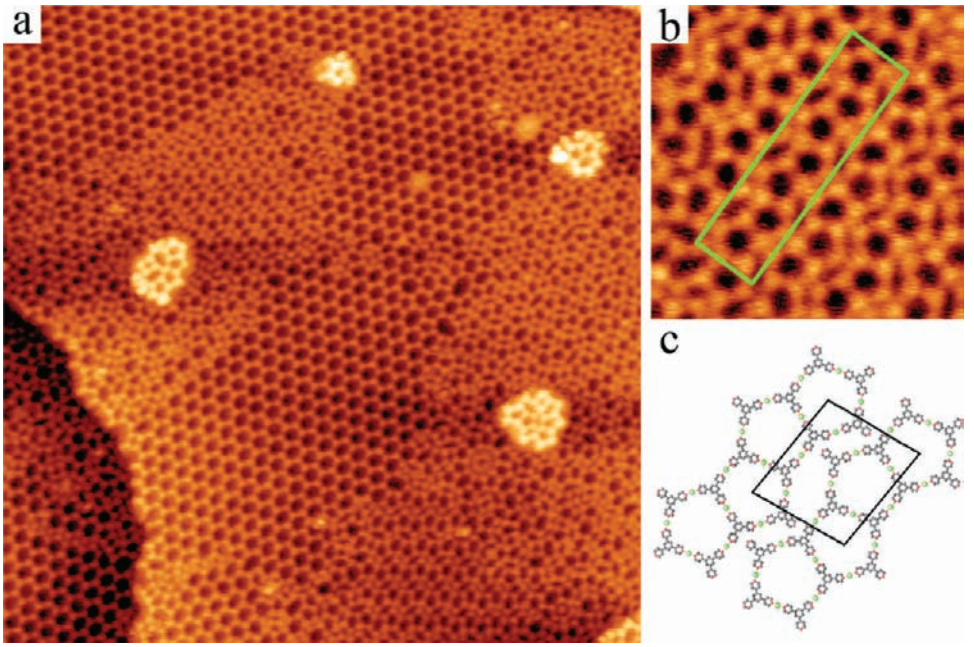

Figure 2. (a) Overview STM topograph (100 × 100 nm) of the TPyB−Cu networks formed at a molecular density of 0.34 TPyB/nm^2. (b) High-resolution image (20 × 20 nm) of the pentagon network. (c) Structural model of the pentagonal network.

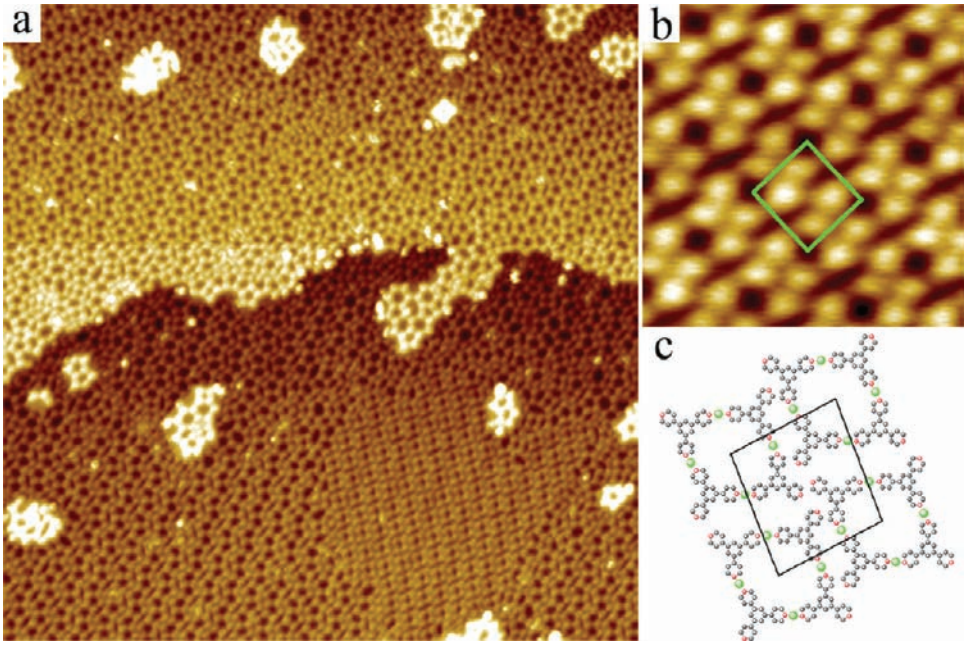

Figure 3. (a) Overview STM topograph (100 nm × 100 nm) of the TPyB−Cu networks formed at a molecular density of 0.38 TPyB/nm^2. (b) High-resolution image (10 nm × 10 nm) of the rhombic cyclic network. (c) Structural model of the rhombic network.

pentagon, five TPyB molecules link with the neighboring molecules in the two-fold Cu−pyridyl coordination. The length of the pentagon side is 2.73 ± 0.05 nm, which is the same as the one of hexagon in the honeycomb network. Among the five molecules, four are involved in the neighboring pentagons and all of their three pyridyl terminal groups participate in coordination. The remaining TPyB molecule in the pentagon only coordinates with two neighboring molecules, while the uncoordinated pyridyl group points toward the benzene core of a TPyB molecule in the adjacent string. The distance between the N atom and the C atom is 0.56 nm, which is beyond the distance of typical hydrogen bonds (0.15−0.35 nm).[19] Thus, the neighboring pentagon strings are likely packed together due to the in-plane compression. In the pentagonal network, a periodic structural unit can be defined by the frame in Figure 2c. On the basis of the STM image, the densities of Cu and TPyB in the network are calculated as 0.50 Cu/nm^2 and 0.37 TPyB/nm^2, which are higher than those in the honeycomb network.

Figure 3a is a typical overview STM topography image of the sample on which the TPyB density is increased to 0.38 TPyB/nm^2.

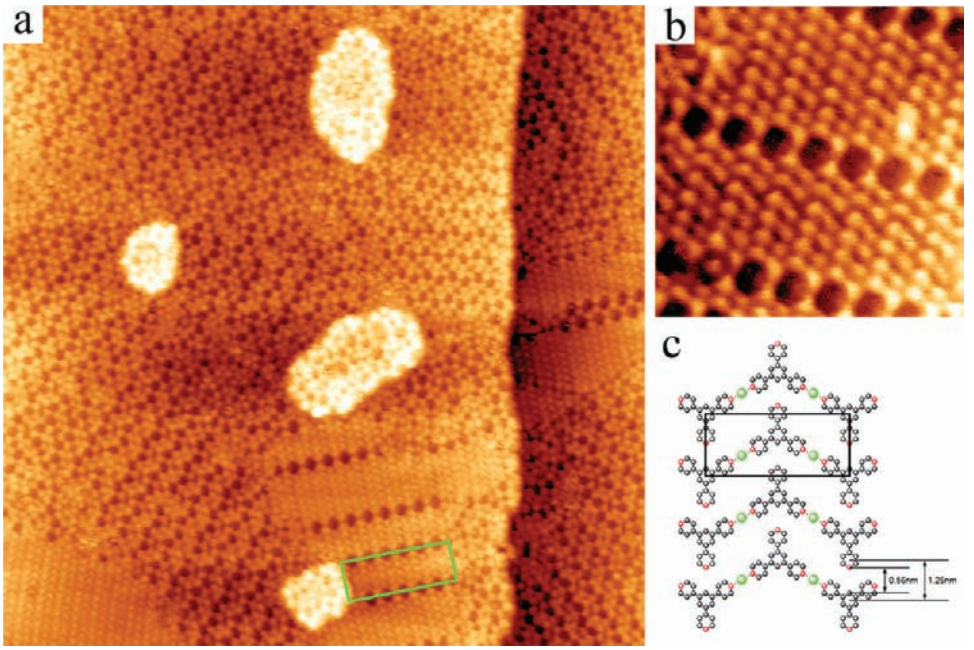

Figure 4. (a) Overview STM topograph (100 nm × 100 nm) of the TPyB−Cu networks formed at a molecular density of 0.40 TPyB/nm^2. (b) High-resolution image (20 nm × 20 nm) of the zigzag phase. (c) Structural model of the zigzag phase.

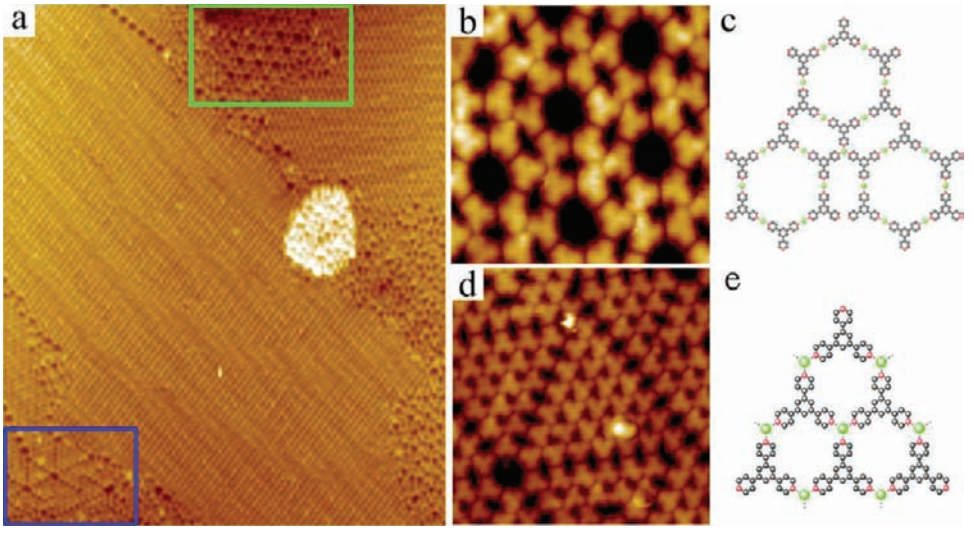

Figure 5. (a) Overview STM topograph (100 nm × 120 nm) of the TPyB−Cu networks formed at a molecular density of 0.47 TPyB/nm^2. (b) High-resolution image (10 nm × 10 nm) of the region marked by the green frame in panel a. (c) Structural model of the phase shown in panel b. (d) High-resolution image (15 nm × 15 nm) of the region marked by the blue frame in panel a. (e) Structural model of the phase shown in panel d.

One can clearly see that the total area of the honeycomb hexagonal networks shrinks remarkably (ca. 1% of TPyB) and the pentagonal networks become dominant (ca. 86% of TPyB). Moreover, a new phase consisting of ordered packing rhombic structures appears (ca. 2% of TPyB). A high-resolution STM image of Figure 3b reveals that each rhombus is composed of four TPyB molecules forming a cyclic unit. In a structural model as shown in Figure 3c, one can see that in a rhombic cycle, four TPyB molecules link with each other in the two-fold Cu−pyridyl coordination. The length of the rhombus side is 2.70/2.98 ± 0.05 nm, which is close to the size of hexagon in the honeycomb network. Each TPyB has one uncoordinated pyridyl ligand that points toward the benzene core of a TPyB molecule in the adjacent rhombic cycle. In this phase, a periodic structural unit can be defined by the frame in Figure 3c. On the basis of the unit cell size, the densities of Cu and TPyB in this phase are calculated as 0.50 Cu/nm^2 and 0.50 TPyB/nm^2.

When further increasing the molecular density to 0.40 TPyB/nm^2, as shown in Figure 4a, the honeycomb and rhombic phases become very few and the pentagonal network phase (ca. 75% of TPyB) is still the main phase. A new structure with densely packed molecules appears in Figure 4a. This new phase consumes about 10% of TPyB. In the high-resolution image of this new phase (see Figure 4b), one may identify here a zigzag-like arrangement of single chains of the TPyB molecules. Figure 4c shows a structural model of the zigzag-chain phase, in which

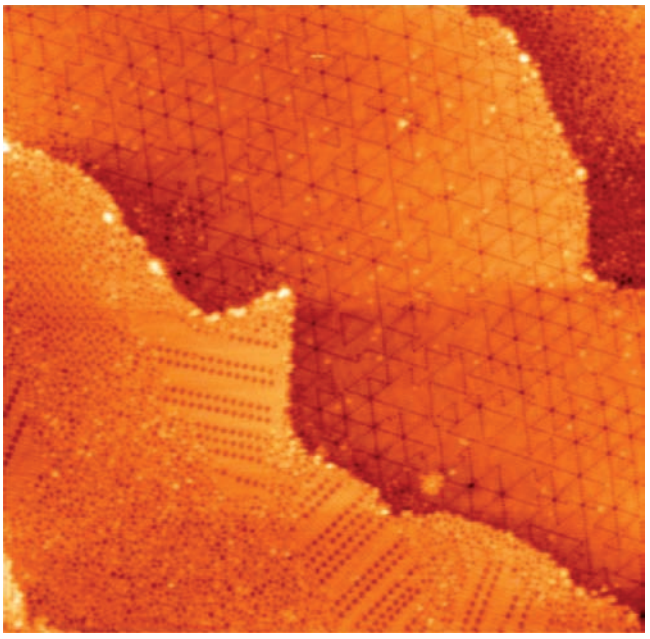

Figure 6. Overview STM topograph (200 nm × 200 nm) showing large area of TPyB−Cu triangular network formed at a molecular density of 0.52 TPyB/nm^2.

Table 1. Molecular Packing Density and Coordination Binding Modes of Each Phase

structure	density (TPyB/nm^2)	coordination bond
honeycomb	0.31	2-fold
pentagon	0.37	2-fold
rhombus	0.50	2-fold
zigzag chain	0.58	2-fold
triangle	0.59	3-fold

every molecule links two neighboring molecules via the two-fold Cu−pyridyl coordination forming the wavy zigzag chains. The remaining uncoordinated pyridyl groups of the TPyB molecules point toward the benzene core of the TPyB molecules of the adjacent chains. The distance between the N atom and the C atom in N···H−C is also 0.56 nm, which again excludes interchain hydrogen bonding, so the zigzag chains are likely packed together due to the in-plane compression. The structural unit of this phase is defined by the rectangle in the model and the unit area is 3.4 nm^2. The packing densities of Cu atom and TPyB molecules in the zigzag-chain phase are 0.58 Cu/nm^2 and 0.58 TPyB/nm^2, higher than those of the open structures of the honeycomb, the pentagonal and the rhombic phases. At even higher molecular density up to 0.50 TPyB/nm^2, the area of the zigzag phase is enlarged and the area of the pentagon phase is reduced, indicating the in-plane compression drives the molecules to form the denser phase.

Figure 5a is a typical STM overview of the sample on which the TPyB density is increased to 0.47 TPyB/nm^2 showing besides the pentagonal phase and the zigzag-chain phase, two new phases emerge as marked by the green frame at the upper and the blue frame at the lower portion of Figure 5a. Figure 5b is a magnified view of the green frame region, where one can see a structure containing hexagonal units connected by rhombic

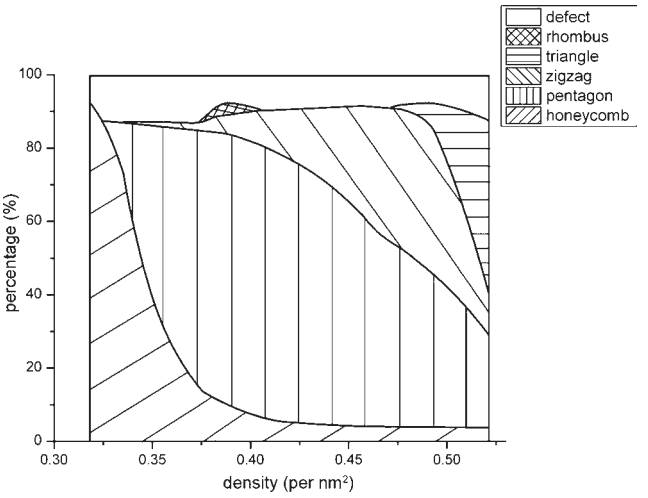

Figure 7. Tentative phase diagram of network structures as a function of molecular density constructed based on the statistical analysis of samples with different molecular coverage.

units. Interestingly, three adjacent hexagons are joined together in a three-fold junction, that is, an arrangement which is identical to the Fe−TPyB network formed on Au(111).[15] The structural model shown in Figure 5c illustrates that the hexagonal and rhombic units contain two-fold Cu−pyridyl coordination, while the three TPyB molecules at three-fold junction coordinate with a central Cu atom in a trigonal configuration. So, Cu atom is in a different coordination from the two-fold Cu−pyridyl coordination pattern in all previous networks. Figure 5d is a magnified view of the blue frame region. It shows a phase of triangular networks in which the three-fold coordination becomes dominant as illustrated in the structural model in Figure 5e. Hexagonal corner holes and linear defect lines exist at the domain boundaries of triangular networks. Each corner of the big triangular lattice is a hexagon which is identical to the honeycomb network unit. According to the STM image, a triangular unit occupies 1.70 nm^2. The densities of Cu atom and TPyB molecules in the triangular network are 0.59 Cu/nm^2 and 0.59 TPyB/nm^2.

Figure 6 is a STM overview of the sample in which the TPyB density is increased to 0.52 TPyB/nm^2 showing that the honeycomb phase disappears, and both the pentagonal phase (ca. 24% of TPyB) and the zigzag-chain phase (ca. 10% of TPyB) are reduced remarkably while the triangular network phase grows larger (ca. 48% of TPyB), as signified by the triangle defect lines. This phenomenon highlights that the alteration of the coordination chemistry of the central metal occurs to accommodate more molecules as the density of the 2D metal−organic coordination network becomes high. Table 1 summarizes the molecular packing density and coordination binding modes of each phase. Obviously, the phases of high molecular packing density appear at the samples in which the molecular density is higher, that is, at higher in-plane compression. To gain quantitative relationship between the molecular density on the surface and the phase transformation, we have analyzed the total amount of TPyB molecules involved in various network structures based on statistical analysis of the STM data of 9 samples providing different molecular densities. Figure 7 presents a tentative diagram showing the phases transformation upon increment of molecular density. The graph illustrates with increment of the molecular density, the most open honeycomb structure is diminished

dx.doi.org/10.1021/ja2056193 |J. Am. Chem. Soc. 2011, 133, 18760–18766

gradually while the less open pentagonal and rhombic, or more densely packed zigzag and trigonal structures become increasingly more dominant. As in the self-assembly processes all molecules are confined in the 2D space, and a high molecular density corresponds to high intrinsic in-plane compression, we propose the observed phase transformation is a consequence of this compression as the transformation to denser network would release the compression effectively. As the molecular density is above 0.47 TPyB/nm^2, some Cu atoms are coordinated in three-fold, which indicates the intrinsic alteration of the coordination chemistry occurs at high molecular density. We have carried out cross-checking experiments to validate the compression-induced structural transformation. In the Cu-deficient case, the honeycomb network phase and close-packed TPyB molecular layer were formed at low molecular density (below the full monolayer of honeycomb phase). In other words, the lack of Cu will not result in those high-packing density phases.

CONCLUSION

In summary, we have investigated the phase transformation of the 2D metal−organic coordination networks driven by in-plane compression. We have found that the honeycomb network is formed at first below full monolayer coverage, and transforms under higher molecular density, that is, high in-plane compression, to the pentagonal networks, rhombic cycles, then to the zigzag structure, and finally to the triangular networks. It is very interesting to find that the Cu−pyridyl binding is in the two-fold coordination configuration in most networks but can be transformed to the three-fold coordination configuration in the triangular network under high molecular density, which illustrates the coordination chemistry of Cu−pyridyl can be altered under high compression. This work demonstrates that a subtle modification of the parameters such as compression can lead to distinctive 2D coordination networks and different coordination chemistry, which offers an alternative route in guiding the 2D supramolecular self-assembly.

EXPERIMENTAL METHODS

Synthesis. TPyB ligand was synthesized according to the reported procedure.[20]

Sample Preparation and STM Measurement. All sample preparations and STM measurements were performed in ultra high vacuum conditions. A single-crystal Au(111) was cleaned by cycles of Ar^+ ion sputtering and annealing to 850 K. Copper atoms were deposited for 10 min using an electron beam metal evaporator on the Au(111) surface held at room temperature and the Cu was assured to be always overdosed as evidenced by the presence of extra Cu islands in all samples. On the same surface, TPyB molecules were deposited at 470 K using an organic molecular beam deposition source. The sample was held at room temperature for all depositions. After the TPyB deposition, the sample was annealed at 420 K. Then, the sample was characterized *in situ* by an Omicron scanning tunneling microscope (STM) at 293 K in the constant current mode (bias voltage = -1.3 V and tunneling current = 0.3 nA). The data analysis was conducted using WSxM software.[21]

AUTHOR INFORMATION

Corresponding Author
liupn@ecust.edu.cn; phnlin@ust.hk

ACKNOWLEDGMENT

This work was supported financially by Hong Kong Research Council Grant No. 602409, the National Natural Science Foundation of China (Project Nos. 20902020, 21172069), the Fundamental Research Funds for the Central Universities and the Innovation Program of Shanghai Municipal Education Commission (12ZZ050).

REFERENCES

(1) For some recent reviews of supramolecular assembly materials: (a) Leong, W. L.; Vittal, J. J. *Chem. Rev.* **2011**, *111*, 688. (b) Kim, H.-J.; Kim, T.; Lee, M. *Acc. Chem. Res.* **2011**, *44*, 72. (c) Gessner, V. H.; Tannaci, J. F.; Miller, A. D.; Tilley, T. D. *Acc. Chem. Res.* **2011**, *44*, 435. (d) Beletskaya, I.; Tyurin, V. S.; Tsivadze, A. Y.; Guilard, R.; Stern, C. *Chem. Rev.* **2009**, *109*, 1659. (e) Qiu, Y.; Chen, P.; Liu, M. *J. Am. Chem. Soc.* **2010**, *132*, 9644. (f) Pashuck, E. T.; Stupp, S. I. *J. Am. Chem. Soc.* **2010**, *132*, 8819. (g) Rabone, J.; Yue, Y.-F.; Chong, S. Y.; Stylianou, K. C.; Bacsa, J.; Bradshaw, D.; Darling, G. R.; Berry, N. G.; Khimyak, Y. Z.; Ganin, A. Y.; Wiper, P.; Claridge, J. B.; Rosseinsky, M. J. *Science* **2010**, *329*, 1053.

(2) For some recent reviews of MOFs: (a) Themed issue: Hybrid materials, *Chem. Soc. Rev.* **2011**, *40*, 453. (b) Themed issue: Metal-organic frameworks, *Chem. Soc. Rev.* **2009**, *38*, 1201. (c) Zhao, D.; Timmons, D. J.; Yuan, D.; Zhou, H.-C. *Acc. Chem. Res.* **2011**, *44*, 123. (d) Farha, O. K.; Hupp, J. T. *Acc. Chem. Res.* **2010**, *43*, 1166. (e) Zacher, D.; Schmid, R.; Wöll, C.; Fischer, R. A. *Angew. Chem., Int. Ed.* **2011**, *50*, 176. (f) Carné, A.; Carbonell, C.; Imaz, I.; Maspoch, D. *Chem. Soc. Rev.* **2011**, *40*, 291. (g) Chen, B.; Xiang, S.; Qian, G. *Acc. Chem. Res.* **2010**, *43*, 1115. (h) Zhang, J.-P.; Huang, X.-C.; Chen, X.-M. *Chem. Soc. Rev.* **2009**, *38*, 2385.

(3) For some recent reviews of STM studied (2D) MOFs: (a) Bartels, L. *Nat. Chem.* **2010**, *2*, 87. (b) Lin, N.; Stepanow, S.; Ruben, M.; Barth, J. V. *Top. Curr. Chem.* **2009**, *287*, 1. (c) Bonifazi, D.; Mohnani, S.; Llanes-Pallas, A. *Chem.—Eur. J.* **2009**, *15*, 7004. (d) Kudernac, T.; Lei, S.; Elemans, J. A. A. W.; De Feyter, S. *Chem. Soc. Rev.* **2009**, *38*, 402. (e) Stepanow, S.; Lin, N.; Barth, J. V. *J. Phys.: Condens. Matter* **2008**, *20*, 184002. (f) Cicoira, F.; Santato, C.; Rosei, F. *Top. Curr. Chem.* **2008**, *285*, 203.

(4) For some reviews related to the phase transformation of (2D) self-assembled monlayer: (a) Liang, H.; He, Y.; Ye, Y.; Xu, X.; Cheng, F.; Sun, W.; Shao, X.; Wang, Y.; Li, J.; Wu, K. *Coord. Chem. Rev.* **2009**, *253*, 2959. (b) Elemans, J. A. A. W.; De Feyter, S. *Soft Matter* **2009**, *5*, 721. (c) Moulton, B.; Zaworotko, M. J. *Chem. Rev.* **2001**, *101*, 1629.

(5) (a) Miao, X.; Xu, L.; Li, Z.; Deng, W. *J. Phys. Chem. C* **2011**, *115*, 3358. (b) Zhang, X.; Chen, T.; Chen, Q.; Deng, G.-J.; Fan, Q.-H.; Wan, L.-J. *Chem.—Eur. J.* **2009**, *15*, 9669. (c) Mamdouh, W.; Uji-i, H.; Ladislaw, J. S.; Dulcey, A. E.; Percec, V.; De Schryver, F. C.; De. Feyter, S. *J. Am. Chem. Soc.* **2006**, *128*, 317. (d) Tahara, K.; Furukawa, S.; Uji-i, H.; Uchino, T.; Ichikawa, T.; Zhang, J.; Mamdouh, W.; Sonoda, M.; De Schryver, F. C.; De Feyter, S.; Tobe, Y. *J. Am. Chem. Soc.* **2006**, *128*, 16613.

(6) (a) Ahn, S.; Matzger, A. J. *J. Am. Chem. Soc.* **2010**, *132*, 11364. (b) Tahara, K.; Okuhata, S.; Adisoejoso, J.; Lei, S.; Fujita, T.; De Feyter, S.; Tobe, Y. *J. Am. Chem. Soc.* **2009**, *131*, 17583. (c) Lei, S.; Tahara, K.; De Schryver, F. C.; Van der Auweraer, M.; Tobe, Y.; De Feyter, S. *Angew. Chem., Int. Ed.* **2008**, *47*, 2964. (d) Kampschulte, L.; Werblowsky, T. L.; Kishore, R. S. K.; Schmittel, M.; Heckl, W. M.; Lackinger, M. *J. Am. Chem. Soc.* **2008**, *130*, 8502. (e) Miao, X.; Xu, L.; Li, Y.; Li, Z.; Zhou, J.; Deng, W. *Chem. Commun.* **2010**, *46*, 8830.

(7) (a) Gutzler, R.; Sirtl, T.; Dienstmaier, J. F.; Mahata, K.; Heckl, W. M.; Schmittel, M.; Lackinger, M. *J. Am. Chem. Soc.* **2010**, *132*, 5084. (b) Merz, L.; Parschau, M.; Zoppi, L.; Baldridge, K. K.; Siegel, J. S.; Ernst, K.-H. *Angew. Chem., Int. Ed.* **2009**, *48*, 1966. (c) English, W. A.; Hipps, K. W. *J. Phys. Chem. C* **2008**, *112*, 2026. (d) Ruben, M.; Payer, D.; Landa, A.; Comisso, A.; Gattinoni, C.; Lin, N.; Collin, J.-P.; Sauvage, J.-P.; Vita, A. D.; Kern, K. *J. Am. Chem. Soc.* **2006**, *128*, 15644. (e) Otero, R.; Xu, W.;

Lukas, M.; Kelly, R. E. A.; Lœgsgaard, E.; Stensgaard, I.; Kjems, J.; Kantorovich, L. N.; Besenbacher, F. *Angew. Chem., Int. Ed.* **2008**, *47*, 9673.

(8) (a) Pivetta, M.; Blüm, M.-C.; Patthey, F.; Schneider, W.-D. *ChemPhysChem* **2010**, *11*, 1558. (b) Otero, R.; Lukas, M.; Kelly, R. E. A.; Xu, W.; Lægsgaard, E.; Stensgaard, I.; Kantorovich, L. N.; Besenbacher, F. *Science* **2008**, *319*, 312. (c) Xu, B.; Tao, C.; Williams, E. D.; Reutt-Robey, J. E. *J. Am. Chem. Soc.* **2006**, *128*, 8493. (d) Poirier, G. E.; Pylant, E. D. *Science* **1996**, *272*, 1145.

(9) (a) Huang, Y.; Chen, W.; Li, H.; Ma, J.; Pflaum, J.; Wee, A. T. S. *Small* **2010**, *6*, 70. (b) Wakayama, Y.; De Oteyza, D. G.; Garcia-Lastra, J. M.; Mowbray, D. J. *ACS Nano* **2011**, *5*, 581. (c) Treier, M.; Nguyen, M.-T.; Richardson, N. V.; Pignedoli, C.; Passerone, D.; Fasel, R. *Nano Lett.* **2009**, *9*, 126.

(10) (a) Mali, K. S.; Wu, D.; Feng, X.; Müllen, K.; Van der Auweraer, M.; De Feyter, S. *J. Am. Chem. Soc.* **2011**, *133*, 5686. (b) Yang, B.; Wang, Y.; Li, G.; Cun, H.; Ma, Y.; Du, S.; Xu, M.; Song, Y.; Gao, H.-J. *J. Phys. Chem. C* **2009**, *113*, 17590. (c) Lei, S.-B.; Deng, K.; Yang, Y.-L.; Zeng, Q.-D.; Wang, C.; Jiang, J.-Z. *Nano Lett.* **2008**, *8*, 1836. (d) Yang, Y.-L.; Chan, Q.-L.; Ma, X.-J.; Deng, K.; Shen, Y.-T.; Feng, X.-Z.; Wang, C. *Angew. Chem., Int. Ed.* **2006**, *45*, 6889. (e) Lu, X.; Polanyi, J. C.; Yang, J. S. Y. *Nano Lett.* **2006**, *6*, 809. (f) Lahann, J.; Mitragotri, S.; Tran, T.-N.; Kaido, H.; Sundaram, J.; Choi, I. S.; Hoffer, S.; Somorjai, G. A.; Langer, R. *Science* **2003**, *299*, 371. (g) Yanagi, H.; Ikuta, K.; Mukai, H.; Shibutani, T. *Nano Lett.* **2002**, *2*, 951.

(11) (a) Blunt, M. O.; Russell, J. C.; Gimenez-Lopez, M. C.; Taleb, N.; Lin, X.; Schröder, M.; Champness, N. R.; Beton, P. H. *Nat. Chem.* **2011**, *3*, 74. (b) Li, Y.; Wan, J.; Deng, K.; Han, X.; Lei, S.; Yang, Y.; Zheng, Q.; Zeng, Q.; Wang, C. *J. Phys. Chem. C* **2011**, *115*, 6540.

(12) Tan, J. C.; Cheetham, A. K. *Chem. Soc. Rev.* **2011**, *40*, 1059.

(13) (a) Spencer, E. C.; Angel, R. J.; Ross, N. L.; Hanson, B. E.; Howard, J. A. K. *J. Am. Chem. Soc.* **2009**, *131*, 4022. (b) Bennett, T. D.; Tan, J.-C.; Moggach, S. A.; Galvelis, R.; Mellot-Draznieks, C.; Reisner, B. A.; Thirumurugan, A.; Allan, D. R.; Cheetham, A. K. *Chem.—Eur. J.* **2010**, *16*, 10684. (c) Moggach, S. A.; Bennett, T. D.; Cheetham, A. K. *Angew. Chem., Int. Ed.* **2009**, *48*, 7087. (d) Kosa, M.; Tan, J.-C.; Merrill, C. A.; Krack, M.; Cheetham, A. K.; Parrinello, M. *ChemPhysChem* **2010**, *11*, 2332.

(14) (a) Chapman, K. W.; Halder, G. J.; Chupas, P. J. *J. Am. Chem. Soc.* **2008**, *130*, 10524. (b) Chapman, K. W.; Halder, G. J.; Chupas, P. J. *J. Am. Chem. Soc.* **2009**, *131*, 17546. (c) Beurroies, I.; Boulhout, M.; Llewellyn, P. L.; Kuchta, B.; Férey, G.; Serre, C.; Denoyel, R. *Angew. Chem., Int. Ed.* **2010**, *49*, 7526.

(15) Shi, Z.; Liu, J.; Lin, T.; Xia, F.; Liu, P. N.; Lin, N. *J. Am. Chem. Soc.* **2011**, *133*, 6150.

(16) (a) Klappenberger, F.; Weber-Bargioni, A.; Auwärter, W.; Marschall, M.; Schiffrin, A.; Barth, J. V. *J. Chem. Phys.* **2008**, *129*, 214702. (b) Tait, S. L.; Langner, A.; Lin, N.; Stepanow, S.; Rajadurai, C.; Ruben, M.; Kern, K. *J. Phys. Chem. C* **2007**, *111*, 10982. (c) Langner, A.; Tait, S. L.; Lin, N.; Rajadurai, C.; Ruben, M.; Kern, K. *Angew. Chem., Int. Ed.* **2008**, *47*, 8835.

(17) Classen, T.; Fratesi, G.; Costantini, G.; Fabris, S.; Stadler, F. L.; Kim, C.; de Gironcoli, S.; Baroni, S.; Kern, K. *Angew. Chem., Int. Ed.* **2005**, *44*, 6142.

(18) (a) Parschau, M.; Fasel, R.; Ernst, K.-H.; Gröning, O.; Brandenberger, L.; Schillinger, R.; Greber, T.; Seitsonen, A. P.; Wu, Y.-T.; Siegel, J. S. *Angew. Chem., Int. Ed.* **2007**, *46*, 8258. (b) Bauert, T.; Merz, L.; Bandera, D.; Parschau, M.; Siegel, J. S.; Ernst, K.-H. *J. Am. Chem. Soc.* **2009**, *131*, 3460. (c) Pivetta, M.; Blüm, M.-C.; Patthey, F.; Schneider, W.-D. *Angew. Chem., Int. Ed.* **2008**, *47*, 1076. (d) Tahara, K.; Balandina, T.; Furukawa, S.; Feyter, S. D.; Tobe, Y. *CrystEngComm* **2011**, *13*, 5551.

(19) Barth, J. V. *Annu. Rev. Phys. Chem.* **2007**, *58*, 375.

(20) Schmittel, M.; He, B.; Mal, P. *Org. Lett.* **2008**, *10*, 2513.

(21) Horcas, I.; Fernández, R.; Gómez-Rodríguez, J. M.; Colchero, J.; Gómez-Herrero, J.; Baro, A. M. *Rev. Sci. Instrum.* **2007**, *78*, 013705.